Metal Ion Substitution in the Catalytic Site Greatly Affects the Binding of Sulfhydryl-Containing Compounds to Leucyl Aminopeptidase[†,‡]

Mario Cappiello,[§,||] Vincenzo Alterio,[||,⊥] Pietro Amodeo,[@] Antonella Del Corso,[§] Andrea Scaloni,[#] Carlo Pedone,[⊥] Roberta Moschini,[§] Gian Marco De Donatis,[§] Giuseppina De Simone,*[,⊥] and Umberto Mura[§]

Department of Physiology and Biochemistry, University of Pisa, I-56126 Pisa, Italy, Institute of Biostructures and Bioimages, CNR, I-80134 Naples, Italy, Institute of Biomolecular Chemistry, CNR, Comprensorio Olivetti, I-80078 Pozzuoli (Naples), Italy, and Proteomics and Mass Spectrometry Laboratory, ISPAAM, CNR, I-80147 Naples, Italy

Received October 11, 2005; Revised Manuscript Received January 18, 2006

ABSTRACT: Bovine lens leucyl aminopeptidase (blLAP), a homohexameric metallopeptidase preferring bulky and hydrophobic amino acids at the N-terminus of (di)peptides, contains two Zn^{2+} ions per subunit that are essential for catalytic activity. They may be replaced by other divalent cations with different exchange kinetics. The protein readily exchangeable site (site 1) can be occupied by Zn^{2+}, Mn^{2+}, Mg^{2+}, or Co^{2+}, while the tight binding site (site 2) can be occupied by Zn^{2+} or Co^{2+}. We recently reported that introduction of Mn^{2+} into site 1 generates a novel activity of blLAP toward CysGly [Cappiello, M., et al. (2004) *Biochem. J. 378*, 35−44], which in contrast is not hydrolyzed by the (Zn/Zn) enzyme. This finding, while disclosing a potential specific role for blLAP in glutathione metabolism, raised a question about the features required for molecules to be a substrate for the enzyme. To clarify the interaction of the enzyme with sulfhydryl-containing derivatives, (Zn/Zn)- and (Mn/Zn)blLAP forms were prepared and functional−structural studies were undertaken. Thus, a kinetic analysis of various compounds with both enzyme forms was performed; the crystal structure of (Zn/Zn)blLAP in complex with the peptidomimetic derivative Zofenoprilat was determined, and a modeling study on the CysGly−(Zn/Zn)blLAP complex was carried out. This combined approach provided insight into the interaction of blLAP with sulfhydryl-containing derivatives, showing that the metal exchange in site 1 modulates binding to these molecules that may result in enzyme substrates or inhibitors, depending on the nature of the metal.

Aminopeptidases catalyze the removal of the N-terminal amino acid from proteins and peptides. They are widely distributed among prokaryotes and eukaryotes, where they are thought to play a fundamental role in protein processing or metabolism of bioactive peptides (*1*). Leucyl aminopeptidase (LAP)[1] is one of the best characterized aminopeptidases with respect to sequence, structure, and mechanism of action. Alterations in LAP activity have been found in a variety of diseases, including cancer (*2*) and cataracts (*3*). An increase in leucyl aminopeptidase activity has also been reported in HIV-infected cells, suggesting that this enzyme may have a role in early events of HIV infection (*4*). Previous studies have shown that LAP from bovine lens (blLAP) is a hexameric enzyme; each of its six identical 54 kDa subunits contains two Zn^{2+} ions in the active site, which are fundamental for catalytic activity and exhibit different metal ion exchange kinetics. The so-called readily exchangeable site (site 1) can be occupied by different metals (M1), Zn^{2+}, Mn^{2+}, Mg^{2+}, or Co^{2+}, while the so-called tight binding site (site 2) can be occupied by only Zn^{2+} or Co^{2+} (M2) (*5*−*7*). It has also been shown that metal substitution in both binding sites greatly affects k_{cat} and K_m values, suggesting that both metal ions play a role in substrate binding and transition state stabilization (*7*). The three-dimensional structure of (Zn/Zn)-blLAP in complex with a series of inhibitors has been determined, allowing for the identification of molecular moieties involved in substrate recognition (*8*−*11*). On the basis of the catalytic mechanism proposed for peptide cleavage by various aminopeptidases, a series of sulfur-containing blLAP inhibitors have been designed and tested for kinetic properties (*12*−*16*). However, these studies produced contradictory results with respect to the capability of these derivatives to strongly interact with metal ions present in the enzyme active site.

Recently, LAP has been identified as the main CysGly hydrolyzing activity in rat liver and bovine eye lens (*17*, *18*); this activity has been related to the presence of the Mn^{2+} ion in site 1 (*17*). In this case, CysGly was reported to be as good a substrate as conventional derivatives containing a bulky hydrophobic amino acid at their N-termini (*19*).

[†] This work was supported by grants from Ministero dell'Istruzione, dell'Università e della Ricerca Scientifica, FIRB2001, Contract RBAU01T97W.

[‡] The coordinates and structure factors of the Zofenoprilat−(Zn/Zn)-blLAP complex have been deposited with the Protein Data Bank as entry 2EWB.

* To whom correspondence should be addressed. Phone: +39-081-2534579. Fax: +39-081-2536642. E-Mail: gdesimon@unina.it.

[§] University of Pisa.

[||] These authors made equal contributions to this work.

[⊥] Institute of Biostructures and Bioimages, CNR.

[@] Institute of Biomolecular Chemistry, CNR.

[#] Proteomics and Mass Spectrometry Laboratory, ISPAAM, CNR.

[1] Abbreviations: LAP, leucyl aminopeptidase; blLAP, bovine lens leucyl aminopeptidase; DTT, dithiothreitol; EDTA, ethylenediaminetetraacetate; MD, molecular dynamics; RA, restrained approach; nPT, constant pressure−temperature; UA, unrestrained approach.

10.1021/bi052069v CCC: $33.50
Published on Web 02/14/2006

Molecular modeling studies describing the interaction of this dipeptide within the (Mn/Zn)enzyme active site provided a molecular explanation for this catalytic behavior (*17*). Although unable to fit into the hydrophobic pocket, otherwise occupied by the bulky side chain of the substrate N-terminal amino acid in the (Zn/Zn)enzyme, CysGly was predicted to be able to accommodate its sulfhydryl group in the (Mn/Zn)blLAP active site by interacting with residue Lys262. These findings disclosed a potential role for this enzyme in glutathione metabolism and raised questions regarding molecular determinants controlling substrate recognition.

To further clarify the effect of the metal substitution on the enzyme catalytic behavior, (Zn/Zn)- and (Mn/Zn)blLAP forms were prepared and comparative functional−structural studies were undertaken. In particular, a kinetic analysis of various sulfur-containing derivatives with both protein forms was performed. A competitive inhibitor specific for LeuGly hydrolase activity of (Zn/Zn)blLAP was identified and cocrystallized with the enzyme. Its determined three-dimensional structure was used as a template for modeling studies of complexes of (Zn/Zn)blLAP with other inhibitors. This combined approach provided definitive insight into the structural features controlling substrate−inhibitor interaction with the enzyme, unveiling how (Mn/Zn)blLAP or (Zn/Zn)-blLAP could alternatively hydrolyze or be inhibited by thiol-containing compounds, respectively.

MATERIALS AND METHODS

Materials. CysGly and dithiothreitol (DTT) were purchased from Sigma (St. Louis, MO). Ninhydrin was from Merck (Darmstadt, Germany). Centricon 30 microconcentrators were from Amicon. All inorganic chemicals were reagent grade and from BDH (Poole, U.K.). Zofenoprilat {[1(*S*),4(*S*)]-1-(3-mercapto-2-methyl-1-oxopropyl)-4-(phenylthio)-L-proline} was a gift from Menarini Ricerche SpA (Pomezia, Italy). Calf eyes were obtained from freshly slaughtered animals at the local slaughterhouse, and the lenses were kept frozen until they were used.

Preparation of (Mn/Zn)blLAP and (Zn/Zn)blLAP. (Mn/Zn)blLAP was purified as previously described (*17*), with minor modifications to improve the yield and enzyme stability. In fact, after ethanol precipitation, 0.02 M instead of 0.1 M magnesium acetate was added, and 10 mM sodium phosphate (pH 7.8) containing 2 mM DTT and 0.05 mM manganese chloride was used as the eluent for chromatographic separation on a Sephacryl S-300 column. These protocol changes allowed us to obtain a 20−25% yield of pure enzyme (final specific activity with CysGly as substrate of 15 units/mg), which was stable for at least 2 months, at −80 °C. (Zn/Zn)blLAP was prepared with the same procedure, except that the eluent for chromatography on the Sephacryl S-300 column was 10 mM sodium phosphate (pH 7.8) containing 2 mM DTT and 0.1 mM zinc sulfate. As already reported for the (Zn/Zn)enzyme (*19*), (Zn/Zn)blLAP had a reduced specific activity on LeuGly and was activated by addition of Mn^{2+} ions (data not shown).

Protein concentrations were estimated by the Coomassie blue binding assay (*20*) with bovine serum albumin as the standard.

Enzyme Assays. CysGly hydrolase activity was assayed by a colorimetric method that measures the produced cysteine, following its reaction with ninhydrin in the presence of an acetic acid/HCl mixture (*17*). Enzymatic activity toward LeuGly was measured following the decrease in absorbance at 225 nm associated with dipeptide hydrolysis. One unit of enzyme activity is defined as the amount of enzyme catalyzing the hydrolysis of 1 μmol of dipeptide per minute, under the assay conditions.

Inhibition Studies. Inhibition studies were performed by varying the concentration of substrates at fixed concentrations of the inhibitor. CysGly concentrations were varied from 0.2 to 2 mM and LeuGly concentrations from 0.25 to 8 mM. The value of the apparent K_i was obtained graphically by plotting the slopes of double-reciprocal plots at different inhibitor concentrations versus the inhibitor concentrations in the case of competitive inhibition or by plotting the *y*-intercepts of double-reciprocal plots at different inhibitor concentrations versus the inhibitor concentrations in the case of noncompetitive inhibition. The intercepts on the *x*-axis of these plots gave the values of K_i (*21*).

Mn^{2+} Dependence of CysGly Hydrolase Activity of blLAP. (Mn/Zn)blLAP was extensively dialyzed by ultrafiltration on Centricon 30 microconcentrators against 10 mM sodium phosphate buffer (pH 8.0) supplemented with 2 mM DTT and 2 mM EDTA and then again dialyzed against the same buffer without EDTA up to a nominal concentration of EDTA of less than 0.01 μM. Aliquots of this preparation were preincubated with different concentrations of $MnCl_2$ (ranging from 0.56 to 400 μM) for 3 h, at 25 °C, and then assayed for CysGly activity.

Crystallization, X-ray Data Collection, and Refinement. Crystals of the Zofenoprilat−(Zn/Zn)blLAP complex were obtained by soaking enzyme crystals (*8*) (hexagonal crystal form, space group $P6_322$) in a solution containing 20 mM Zofenoprilat in the crystallization buffer. A complete data set was collected at 1.85 Å resolution from a single crystal, at 100 K, at Synchrotron source Elettra in Trieste, using a Mar CCD detector. Diffracted intensities were processed using the HKL crystallographic data reduction package (Denzo/Scalepack) (*22*). A total of 409 593 reflections were measured (unit cell parameters, $a = 128.94$ Å, $b = 128.94$ Å, and $c = 119.79$ Å) and reduced to 50 083 unique reflections (completeness, 99.9% in the 20.00−1.85 Å resolution range; *R*-sym = 9.1%). Data processing statistics are given in Table 1.

The structure of the Zofenoprilat−(Zn/Zn)blLAP complex was analyzed by difference Fourier techniques, using PDB entry 1LAM (*8*) as a starting model for refinement. Water molecules were removed from the starting model prior to structure factor and phase calculations. Crystallographic *R*-factor and *R*-free, calculated in the 20.00−1.85 Å resolution range, based on the starting model coordinates, were 0.350 and 0.344, respectively. Fourier maps calculated with $3F_o - 2F_c$ and $F_o - F_c$ coefficients exhibited prominent electron density features in the active site region. After an initial refinement, limited to the enzyme structure (*R*-factor = 0.241 and *R*-free = 0.258), a model for the inhibitor molecule was easily built up and introduced into the atomic coordinate set for further refinement, which proceeded to convergence with continuous map inspections and model updates. Refinement was carried out using CNS (*23*); model building and map inspections were performed using O (*24*). Final crystallographic *R*-factor and *R*-free values calculated

Table 1: Data Collection and Refinement Statistics

data collection (20.00−1.85 Å)	
temperature (K)	100
total no. of reflections	409593
no. of unique reflections	50083
completeness (%)	
overall	99.9
outermost data shell	100.0
R-sym[a] (%)	
overall	9.1
outermost data shell	24.7
mean $I/\sigma(I)$	
overall	22.0
outermost data shell	9.2
refinement statistics (20.00−1.85 Å)	
R-factor[b] (%)	15.6
R-free[c] (%)	17.7
rmsd from ideal geometry	
bond lengths (Å)	0.005
bond angles (deg)	1.29
no. of protein atoms	3715
no. of water molecules	478
average *B* factor (Å^2)	15.7

[a] $R_{sym} = \sum|I_i - \langle I\rangle|/\sum I_i$, over all reflections. [b] *R*-factor $= \sum|F_o - F_c|/\sum F_o$. [c] R_{free} was calculated with 5% of the data withheld from the refinement.

for the 48 946 observed reflections (in the 20.00−1.85 Å resolution range) were 0.177 and 0.156, respectively. The refined model included 3736 complex atoms, 21 atoms belonging to the inhibitor, and 478 water molecules. The rms deviations from ideal values of bond lengths and bond angles (*25*) were 0.005 Å and 1.29°, respectively. The average temperature factor (*B*) for all atoms was 15.7 Å^2. The stereochemical quality of the model was assessed by Procheck (*26*). The most favored and additionally allowed regions of the Ramachandran plot contained 100% of the non-glycine residues. The statistics for refinement are summarized in Table 1.

Molecular Dynamics Simulations. Calculations were performed with the Sander module of AMBER 6.0 (*27*), with AMBER all-atom 1994 parametrization (*28*). Monomers of LAP complexes with CysGly or Zofenoprilat were solvated with the LEaP module of AMBER 6.0 (*27*, *28*) in rectangular boxes of TIP3 water molecules (*29*), whose sizes were chosen by using a clearance of 10 Å in each direction after addition of seven Na^+ ions to ensure electrostatic neutrality and a "closeness" parameter value of 1.0. They underwent an initial round of constrained EM (1000 steps), constrained constant volume−temperature molecular dynamics (MD) (120 ps), and constrained constant pressure−temperature (nPT) MD (80 ps) equilibration.

To evaluate potential problems of time stability and/or geometric distortion of metal coordination, previously observed in MD studies on complexes including doubly or triply charged ions (especially in multinuclear centers) (*30*−*32*) and currently undergoing intensive methodological investigation, we performed a double approach based either on fixing the relative orientations of Zn^{2+} ions and their blLAP ligands, thus allowing local rearrangement of noncovalent ligands only (restrained approach, RA, assuming the exact knowledge of the metal coordination for the complex under examination and preventing any dynamic system characterization), or on gradually freeing all atoms, ending with a totally unrestrained simulation (unrestrained approach, UA, potentially affected by stability problems).

RA trajectory was obtained from an unconstrained nPT MD production run (1 ns) with harmonic restraints on (Zn/Zn)blLAP−ligand atom distances, using reference distance values equal to those detected in the crystallographic structure of the Zofenoprilat−(Zn/Zn)blLAP complex and force constant values of 5 kcal mol^{-1} Å^{-2}. Subsequently, restraints were gradually removed in 100 ps, and a final unrestrained/unconstrained nPT MD production simulation (1 ns) was run, thus providing UA trajectory. Coordinates, velocities, and energies in both production runs were collected every 500 steps for analysis. The last 500 ps of each production MD was subjected to subsequent analysis. MD in a solvent box was run with a dielectric constant ϵ of 1 and a cutoff radius of 8 Å for nonbonded interactions and the particle mesh Ewald description of long-range electrostatic interactions (*33*) (charge-grid density of 0.95 Å, cubic spline interpolation, and a direct sum tolerance of 10^{-5}). Covalent bonds involving hydrogen atoms were constrained by the SHAKE algorithm, which allowed the use of a 1.5 fs integration time step. Simulations were performed in the nPT ensemble ($T = 300$ K and $p = 1$ atm). AMBER 6.0 modules and MOLMOL (*34*) were used for structural analysis.

Monitoring of several geometrical parameters involving the coordination sites indicated for both complexes the occurrence of severe (>0.5 Å) distortions of Zn^{2+}−Zn^{2+} distances at the end of the full equilibration time of both UA simulations. In contrast, all Zn^{2+}−ligand geometric parameters were quite stable for all 1 ns unrestrained simulations and exhibited an only <0.1 Å shortening in comparison with corresponding distances in experimental complexes. This small but systematic deviation, by accumulation of errors on both sides of the blLAP active site, could be the origin of the observed elongation of the Zn^{2+}−Zn^{2+} distance. However, observed Zn^{2+} complexation and H-bond patterns for Zofenoprilat and CysGly were fortunately unaffected by these distortions, as the same binding modes were observed for each ligand in RA and UA simulations. In addition, preferred Zofenoprilat binding in both approaches coincided with that experimentally observed, thus supporting an at least semiquantitative interpretation of our simulations.

RESULTS

Mn^{2+} Dependence of the CysGly Hydrolase Activity of blLAP. The removal of metal ion from the blLAP readily exchangeable site (see Materials and Methods) resulted in the abolition of the CysGly hydrolase activity of the enzyme. blLAP regained CysGly hydrolase activity after preincubation in the presence of $MnCl_2$ (Figure 1) but did not recover this activity in the presence of $ZnSO_4$ at concentrations up to 0.2 mM (data not shown). From the data in Figure 1, an apparent K_{50} (i.e., the concentration of Mn^{2+} necessary to obtain half-maximal reactivation) of 0.56 ± 0.14 μM was obtained by nonlinear regression analysis.

Kinetic Analysis. To clarify the influence of the metal present at site 1 on the enzyme's ability to efficiently interact with sulfhydryl-containing compounds, we comparatively evaluated the functional properties of (Zn/Zn)- and (Mn/Zn)-blLAP. CysGly, a good substrate of the (Mn/Zn)enzyme, was tested as an inhibitor of LeuGly hydrolase activity of (Zn/Zn)blLAP. This dipeptide was not hydrolyzed by (Zn/Zn)-

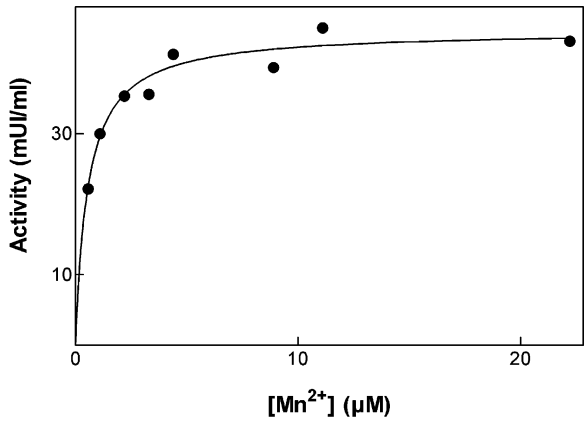

FIGURE 1: Mn^{2+} dependence of CysGly hydrolase activity of blLAP. blLAP (0.75 unit/mL) was treated as described in Materials and Methods for the removal of metal ion from the readily exchangeable site. Aliquots of this preparation were preincubated with different concentrations of $MnCl_2$ (ranging from 0.56 to 400 μM) for 3 h, at 25 °C, and then assayed for CysGly activity. A V_{max} value of 44.6 ± 0.2 milliunits/mL was obtained by nonlinear regression analysis of the data.

Table 2: Inhibition Pattern of (Zn/Zn)- and (Mn/Zn)blLAP

enzyme	substrate	inhibitor	type of inhibition	K_i (μM)
(Mn/Zn)blLAP	CysGly	Zofenoprilat	noncompetitive	1320 ± 170
(Mn/Zn)blLAP	LeuGly	Zofenoprilat	noncompetitive	1080 ± 190
(Mn/Zn)blLAP	CysGly	LeuGly	competitive	650 ± 10
(Zn/Zn)blLAP	LeuGly	Zofenoprilat	competitive	0.8 ± 0.2
(Zn/Zn)blLAP	LeuGly	CysGly	competitive	16.4 ± 4.1

blLAP and revealed a competitive inhibitory action, with a K_i value of 16.4 μM (Table 2). To ascertain the role of the CysGly sulfhydryl group in its inhibitory properties toward the (Zn/Zn)blLAP form, other sulfur-containing derivatives were also evaluated (data not shown). Among these, Zofenoprilat, a peptidomimetic derivative used as an effective and powerful inhibitor of angiotensin converting enzyme (*35*), was found to present efficient inhibitory properties with respect to other nonpeptidic compounds. Like CysGly, Zofenoprilat revealed a competitive inhibitory action with respect to the LeuGly hydrolase activity of (Zn/Zn)blLAP, with a K_i value of 0.8 μM (Table 2). On the other hand, when Zofenoprilat was tested on (Mn/Zn)blLAP, kinetic analyses of inhibition revealed an apparent noncompetitive type of action, with K_i values of 1.3 and 1.1 mM for CysGly and LeuGly used as substrates, respectively (Table 2). The possibility that the apparent noncompetitive behavior of Zofenoprilat could arise from a slow off-rate compared to the time scale of the activity assay was taken into account but was ruled out. In this regard, (Mn/Zn)blLAP was preincubated with 2 mM Zofenoprilat, at 37 °C, for 20 min and then immediately assayed after 5-fold dilution. Under these conditions, the preincubated enzyme exhibited the same extent of inhibition of an enzyme sample preincubated without Zofenoprilat and then assayed in the presence of 0.4 mM inhibitor. Finally, the CysGly hydrolase activity of (Mn/Zn)blLAP was competitively inhibited by LeuGly, with a K_i value of 0.65 mM (Table 2). These kinetic data clearly showed the competitive inhibitory action of (Mn/Zn)blLAP thiol-containing substrates toward (Zn/Zn)blLAP, highlighting the ability of Zofenoprilat to competitively inhibit (Zn/Zn)blLAP.

The molecular bases responsible for the competitive inhibitory properties of sulfhydryl-containing compounds toward (Zn/Zn)blLAP were then investigated. In particular, we determined the crystal structure of the Zofenoprilat−(Zn/Zn)blLAP complex; this inhibitor was chosen because of its stronger affinity for the enzyme. This structure was used as a template for modeling studies on the CysGly−(Zn/Zn)blLAP complex, further refined by molecular dynamics approaches.

Crystallographic Studies. The Zofenoprilat−(Zn/Zn)blLAP complex was prepared and crystallized as described in Materials and Methods. The three-dimensional structure was analyzed by difference Fourier techniques, the crystals being isomorphous to those obtained for the native (Zn/Zn)blLAP (*8*). Inspection of the electron density in the enzyme active site, at various stages of the crystallographic refinement, showed features compatible with the presence of a molecule bound to the active site. The Zofenoprilat structure conformed perfectly to the shape of this electron density (Figure 2a). The main protein−inhibitor interactions are depicted schematically in Figure 2b. According to this figure, the inhibitor molecule presented a peculiar spatial arrangement with respect to the structure of the inhibitor−(Zn/Zn)blLAP complexes described previously (*8*−*11*). In particular, the Zofenoprilat molecule presented the sulfhydryl S atom coordinating both metal ions. On the other hand, the carbonylic oxygen of the inhibitor was hydrogen bonded to the Lys262 NE atom (2.74 Å), while its carboxylate group was exposed to the solvent. Finally, the prolyl and phenyl moieties of Zofenoprilat were stabilized by a large number of strong van der Waals interactions (<4.5 Å) with residues Asn330, Asp332, Ala333, Arg336, and Ile421. Binding of Zofenoprilat to the (Zn/Zn)blLAP active site did not significantly perturb the enzyme structure, even in the proximity of the ligand. As a matter of fact, the rms deviation, calculated over all the Cα atoms of the Zofenoprilat−(Zn/Zn)blLAP complex with respect to the unbound enzyme, was 0.36 Å. Interactions between the protein and two zinc ions were entirely preserved. In particular, both metal ions were coordinated by five ligands in the first coordination sphere, with a metal−metal distance of 3.1 Å.

Figure 3 shows a structural overlay of (Zn/Zn)blLAP bound to Zofenoprilat, amastatin, LeuP, and leucinal, as determined by the superposition of blLAP active site residues. This figure clearly shows that the sulfhydryl S atom of Zofenoprilat presented a position that was very close to that of the bridging OH group of the other bound inhibitors in the corresponding structures. However, as opposed to amastatin−, LeuP−, and leucinal−enzyme complexes that all presented Zn^{2+} in site 2 ($Zn^{2+}2$) as a hexacoordinated ion, the Zofenoprilat−(Zn/Zn)blLAP complex exhibited a pentacoordination for this ion, as in the case of the unbound enzyme. Hexacoordination was due to the presence of the N-terminal amino acid nitrogen atom of amastatin, LeuP, and leucinal, not present in the Zofenoprilat structure. Moreover, as in the unbound enzyme, a Zn^{2+}−Zn^{2+} distance of 3.1 Å was observed for the Zofenoprilat−(Zn/Zn)blLAP complex; this distance was 3.3, 3.4, and 3.2 Å in amastatin−, LeuP−, and leucinal−enzyme complexes, respectively.

Ab initio energy minimization of the Zofenoprilat structure detected in its enzyme complex showed that this conformation substantially corresponded to a stable Zofenoprilat

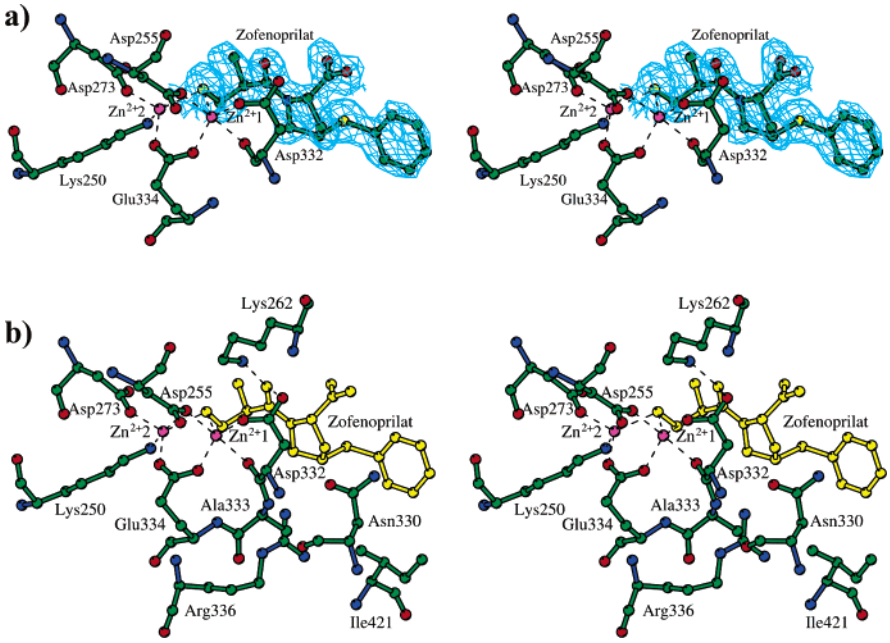

FIGURE 2: Stereoview of the active site region in the Zofenoprilat−(Zn/Zn)blLAP complex. (a) A simulated annealing omit $|2F_o - F_c|$ electron density map (*23*), relative to the inhibitor molecule, is shown. (b) Residues coordinating the two metal ions and participating in recognition of the inhibitor molecule are reported. Hydrogen bonds are shown.

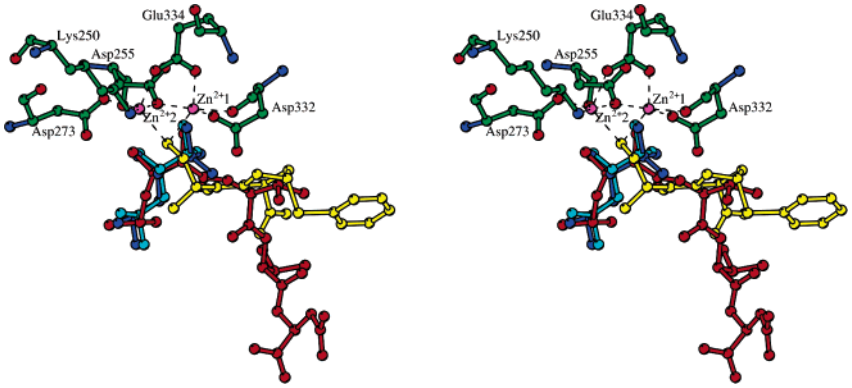

FIGURE 3: Stereoview of the (Zn/Zn)blLAP active site in the presence of Zofenoprilat (yellow), amastatin (red) (PDB entry 1BLL), leucinal (cyan) (PDB entry 1LAN), and LeuP (blue) (PDB entry 1LCP) brought to optimal structural overlay.

conformer, with the exception of its CH_2-S moiety. In fact, observed changes in the $\chi(N-C-C-CH_2)-\chi(C-C-CH_2-S)$ dihedral angle pair from 96° and 52° (crystallographic complex structure) to 138° and 75° or 89° and −168°, respectively (ab initio structures of isolated mono- and dianionic forms, respectively), only determined a rotation of the CH_2-S moiety with respect to the Zofenoprilat backbone. While these combined values in the ab initio monoanionic conformer still kept the S atom ∼1.8 Å from its position in the crystallographic structure, this distance almost doubled (3.4 Å) in the ab initio dianionic structure to minimize electrostatic repulsion between S and amide/carboxylate O atoms. These overall results strongly suggested that the van der Waals interactions mentioned above between Zofenoprilat prolyl/phenyl moieties and several hydrophobic blLAP residues did not affect the intrinsic conformational preference of Zofenoprilat. In contrast, interactions with enzyme Zn^{2+} ions seemed to be sufficiently strong to locally perturb the Zofenoprilat conformation. Moreover, the observed relative position of the thiol group suggested its occurrence either in a protonated state or in a partially negatively charged form with a net reduction of its charge density upon interaction with neighboring atoms. Both findings supported the hypothesis of a large contribution of this S atom in binding of Zofenoprilat to blLAP.

Modeling Studies. The possible occurrence of a different mode of binding of CysGly to (Zn/Zn)blLAP, due to the presence of the N-terminal amino acid nitrogen atom, was investigated by modeling and molecular dynamics approaches. The CysGly molecule was docked in the (Zn/Zn)-blLAP active site using as a template the coordinates of the enzyme−Zofenoprilat complex.

The structural and energetic features of Zofenoprilat− and CysGly−(Zn/Zn)blLAP complexes were compared by a simulation with a MD approach in explicit solvent. In the case of Zofenoprilat, the bicarbonate ion observed in the crystallographic structure of this complex was also included. To extend equilibration and simulation times, monomers of the two complexes, rather than hexamers, were simulated. A comparison of the final UA structure of the Zofenoprilat complex with the corresponding crystallographic structure showed that rmsd values of 0.62, 0.31, and 0.42 Å were detected after 1 ns of MD on selected backbone (403 residues, excluding two terminal residues at each end and

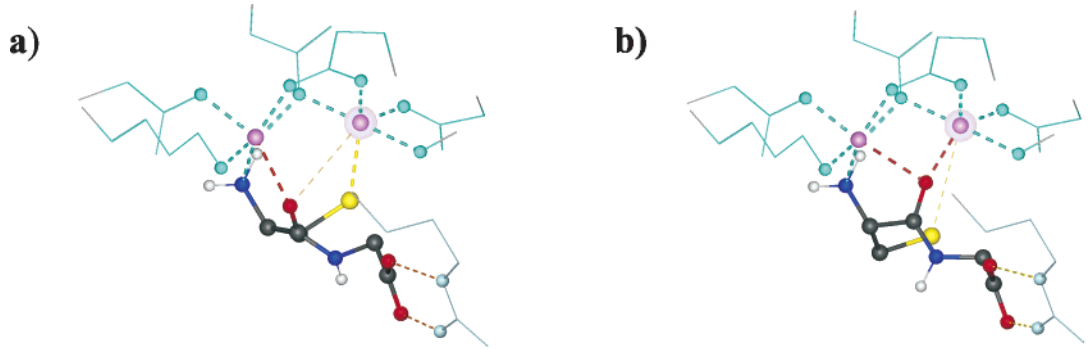

FIGURE 4: Models of the CysGly−(Zn/Zn)blLAP (a) and CysGly−(Mn/Zn)blLAP (b) complexes from MD simulations. The following atoms and bonds are shown: blLAP backbone bonds (light blue lines), side chain heavy atom bonds of residues coordinating the two metal ions (cyan sticks with spheres for metal binding atoms), Arg336 side chain (light blue sticks, with spheres indicating atoms involved in the H-bond with CysGly), metal ions (pink spheres), and heavy atom plus polar hydrogen bonds of CysGly (ball and stick, colored per atom type). Thick dashed sticks (colored cyan when coincident in both models and according to ligand color in other cases) represent metal coordination interactions, and thin dashed sticks represent lost ion interactions in the model. Medium dashed lines represent H-bonds between C-terminal oxygens of CysGly and Arg336. A pink transparent sphere surrounds the LAP exchangeable ion site.

eight flexible loops), active site backbone, and all heavy active site atoms, respectively. A general result of MD simulations for both Zofenoprilat− and CysGly−(Zn/Zn)-blLAP complexes was the ligand mobility and flexibility observed inside the enzyme active site. However, while in the case of Zofenoprilat this dynamic feature derived mostly from the presence of a single (although bifurcated) anchoring site for the Zn^{2+}−Zn^{2+} dinuclear complex, for CysGly this ligand mobility mainly depended on the lack of those bulky hydrophobic groups characterizing the best natural LAP substrates and synthetic ligands. This combination of mobility and flexibility induced fluctuations also in Zn^{2+} complexation, in particular for S atoms, oscillating between mono- and bidentate Zn^{2+} coordination patterns. However, while the bidentate Zn^{2+}−S−Zn^{2+} form represented more than 90% of the population for the Zofenoprilat−(Zn/Zn)blLAP complex, a monodentate interaction with Zn^{2+} in site 1 (Zn^{2+}1) occurred in more than 95% of the CysGly−(Zn/Zn)blLAP complex structures that were sampled. The observed coincidence of crystallographic and calculated model structures for the Zofenoprilat−(Zn/Zn)blLAP complex validated our MD simulation approach, thus ensuring the reliability of the calculated CysGly−(Zn/Zn)blLAP complex model. For this latter complex, the most frequently represented (>75% of simulated time) CysGly arrangement inside the enzyme active site exhibited three coordinating interactions with Zn^{2+} ions (Figure 4a). In addition to the binding of Zn^{2+}1 through the S atom, N-terminal nitrogen atom and Cys carbonylic O atom interactions with Zn^{2+}2 were also observed. The latter interactions also occurred for other inhibitors complexed to blLAP and are assumed to contribute to binding and activation mechanisms of blLAP substrates. However, the simultaneous occurrence of the S atom in the Zn^{2+}1 coordination site displaced the water (or OH^-) molecule playing a fundamental role in all proposed peptide bond hydrolyzing mechanisms (*36*). At the same time, this interaction moved the Cys carbonylic O atom toward Zn^{2+}2 and away from the symmetrical bridging coordination site also observed in models of the LeuGly−(Zn/Zn)blLAP complex (data not shown), increasing the Zn^{2+}−Zn^{2+} distance of 0.2−0.4 Å. Finally, the CysGly−(Zn/Zn)blLAP complex was stabilized by an H-bond interaction between the peptide C-terminal carboxylate group and the Arg336 guanidinium group.

Previously reported modeling studies (*17*) showed that CysGly exhibited a completely different behavior when bound to (Mn/Zn)blLAP, showing a dipeptide orientation within the enzyme active site, which strongly resembled the orientation observed for amastatin, LeuP, and leucinal in the corresponding complexes with (Zn/Zn)blLAP. In particular, the dipeptide amino-terminal group was coordinated to Zn^{2+}2 (Cys N−Zn^{2+} distance of 2.20 Å), while the carbonylic oxygen strongly interacted with both catalytic ions (Cys O−Mn^{2+} distance of 2.20 Å and Cys O−Zn^{2+} distance of 2.45 Å) (Figure 4b).

DISCUSSION

Metalloaminopeptidases are ubiquitous enzymes which play a key role in the modification, degradation, and metabolism of protein/peptide substrates. They utilize conserved amino acid residues to generate a scaffold capable of binding one or two metal ions. Biochemical and crystallographic analyses have indicated that for some of these enzymes two metal ions are required for full activity (*1*). In other instances, only a single metal ion is essential for catalysis, while the second metal modulates activity either positively or negatively (*1*). These mononuclear and cocatalytic binuclear metal centers mediate catalysis by providing sites for substrate binding, activating the nucleophile of the reaction, and stabilizing the reaction transition state (*36*). blLAP is an aminopeptidase hydrolyzing substrates with large hydrophobic residues (Leu, Met, Ile, and Val) in position P1 (*36*). Crystallographic investigations have confirmed the occurrence of two nonequivalent metal ions within the enzyme active site, occupying sites with different affinities (M1 and M2) (*37*). Both metal ions are essential for catalytic activity. Metals are liganded in a distorted trigonal-pyramidal coordination sphere by residues Asp255, Asp332, and Glu334 (M1) and Lys250, Asp255, Asp273, and Glu334 (M2), respectively. In (Zn/Zn)blLAP, a water molecule was found to bridge metal ions. Hydrogen bonding interactions occur from this bridging molecule to Lys262 via an intervening solvent molecule and to Arg336 through a bicarbonate ion. This interaction facilitates the generation of a nucleophile solvent molecule within the active site, allowing effective functioning of the enzymatic catalytic machinery. Moreover, crystallographic studies of various inhibitor−(Zn/Zn)blLAP complexes and mutational investigations demonstrated the

direct interaction of Lys262 and M1 with the P1 carbonyl substrate and the subsequent stabilization of the reaction transition state. On the other hand, M2 was shown to interact with the N-terminus of the substrate (*8*−*11*). The differences in binding affinities of M1 and M2 in blLAP allowed the sequential addition of metal ions (Zn^{2+}, Mn^{2+}, Mg^{2+}, Ni^{2+}, and Co^{2+}) and the creation of metallohybrids. Kinetic analysis of different metallohybrids showed the complex effects of metal substitution on activity toward different substrates. Thus, the addition of Mg^{2+} or Mn^{2+} to blLAP containing either Zn^{2+} or Co^{2+} in site 2 resulted in enzyme activation, with a 10-fold increase in the k_{cat} and k_{cat}/K_m values for Leu-containing substrates (*36*).

We recently reported that blLAP can hydrolyze CysGly with a catalytic efficiency similar to that observed for peptides usually considered good substrates (*17*). The CysGly hydrolase activity of blLAP is strictly dependent on Mn^{2+} (Figure 1). To further clarify the effect of the metal substitution in site 1, the kinetic properties of both (Zn/Zn)- and (Mn/Zn)blLAP forms with respect to sulfur-containing compounds were comparatively evaluated in this study. Our experiments showed that metal exchange in site 1 dramatically alters enzyme specificity, transforming (Mn/Zn)blLAP substrates in competitive inhibitors of (Zn/Zn)blLAP. From our kinetic results emerged the ability of an angiotensin-converting enzyme inhibitor, namely, Zofenoprilat, to competitively inhibit (Zn/Zn)blLAP.

Resolution of the crystal structure of the Zofenoprilat−(Zn/Zn)blLAP complex provided an explanation for the poor hydrolyzing activity of (Zn/Zn)blLAP toward Cys-containing substrates. In fact, in this complex, the S atom of the inhibitor coordinates both metal ions occupying a position that is very close to that held in the native structure by the water molecule essential for the hydrolysis mechanism. These data were further confirmed by modeling studies on the CysGly−(Zn/Zn)blLAP complex. In this case, although the Cys S atom coordinated only a single Zn^{2+} ion in the enzyme active site with respect to that observed for Zofenoprilat−(Zn/Zn)-blLAP complex, the presence of the S atom at the $Zn^{2+}1$ coordination site similarly displaced the water molecule fundamental for catalysis and did not allow a CysGly orientation within the enzyme active site that is productive for dipeptide hydrolysis. In conclusion, both crystallographic and modeling data support the hypothesis that the presence of a Zn^{2+} ion in the readily exchangeable site, as a result of its great affinity for the sulfur atom, does not allow an orientation effective for the hydrolysis of S-containing compounds (Figure 4a). In contrast, the occurrence in site 1 of a Mn^{2+} ion, which prefers oxygen or nitrogen-containing ligands, does allow a productive orientation of the sulfur-containing compounds (*17*) (Figure 4b), thus determining their transformation into good substrates.

Examples of changes in substrate specificity upon metal substitution are abundant in the literature (*38*−*40*). However, in most cases, significant quantitative variations in k_{cat} and K_m values for various substrates were observed, although examples of a totally new enzymatic activity have not yet been reported. In this sense, the on−off mechanism here reported for (Mn/Zn)blLAP and (Zn/Zn)blLAP with Cys-containing substrates seems worth mentioning. In general, changes in substrate specificity seem to be related to subtle structural modifications in enzyme active sites upon metal substitution, and not to a specific affinity of the metal for a particular coordinating species (*39*, *40*). The structure of (Mn/Zn)blLAP in comparison with that of the (Zn/Zn) form would definitively provide valuable information about the metal site and shed light on substrate and inhibitor specificity among the metal-substituted blLAP forms (*38*).

A careful evaluation of the data reported in the literature about the dissociation constants measured for the readily exchangeable site of blLAP ($K_{Mn^{2+}}/K_{Zn^{2+}} = 35$) (*41*) and the intracellular Zn^{2+} and Mn^{2+} concentration values in various tissues (*42*−*46*) suggests that the most abundant enzyme form is probably (Zn/Zn)blLAP. However, independent from the relative amount of the two blLAP forms, a specific cysteinylglycine-hydrolyzing activity was clearly measured in lens homogenates, purified, and identified as being associated with (Mn/Zn)blLAP (*17*). The biological relevance of our findings was confirmed by a parallel investigation of Josch and co-workers, which reported a blLAP-catalyzed cysteinylglycine-hydrolyzing activity also in rat liver (*18*). This activity, although probably associated with the limited amount of (Mn/Zn)blLAP present in both tissues with respect to the total (Zn/Zn)blLAP content, was significant and essential in controlling the concentration of an important molecule with pro-oxidant properties, namely, cysteinylglycine. The observation that blLAP can exhibit different enzymatic activities, depending on metal ion nature, suggests that this enzyme could have multiple roles in many normal and physiopathological processes. In fact, the subtle equilibrium between cationic species in the various tissues could inhibit or facilitate LAP enzymatic activity toward specific substrates with respect to others. Recent studies reported an increase in the Zn^{2+} concentration (*43*−*45*) and a decrease in the Mn^{2+} concentration in cataractous lenses (*46*). These findings, together with the observation that an abnormal blLAP activity is strongly correlated to cataract development (*3*), seem to suggest that the catalytic activity of (Mn/Zn)-blLAP toward CysGly may play a role in preventing cataractogenesis. In fact, it has been suggested that abnormal CysGly levels may determine a pro-oxidant activity, thus affecting protein redox status and altering lens functioning (*47*, *48*). This hypothesis is supported by the recent observations that an unbalanced redox potential can determine cataractogenesis (*49*). Thus, an enzyme capable of catabolizing CysGly, namely, (Mn/Zn)blLAP, could play a fundamental role in lens redox regulation. Finally, increased plasma levels of CysGly have been recently reported to be associated with protease inhibition (*50*). The clinical consequences as well as the involvement of (Mn/Zn)blLAP in this alteration of thiol metabolism remain to be further investigated.

ACKNOWLEDGMENT

We thank Sincrotrone Trieste CNR/Elettra for giving us the opportunity to collect data at the Crystallographic Beamline. We are indebted to Dr. G. Pasqualetti and Dr. R. Di Sacco (veterinary staff of Consorzio Macelli S. Miniato, Pisa, Italy) for their valuable cooperation in bovine lens collection. Thanks are also due to Dr. L. Trampetti for her helpful assistance in LAP purification, to Prof. P. G. De Benedetti and Dr. F. Fanelli (Department of Chemistry, University of Modena and Reggio Emilia) for kindly providing CPU time on their Opteron cluster, to AMD Italy

SpA for generous hardware contribution, and to Dr. E. Santori (Italtech Solutions SpA) for technical assistance to the ICB Opteron cluster.

REFERENCES

1. Taylor, A. (1993) Aminopeptidases: Structure and function, *FASEB J. 7*, 290−298.
2. Umezawa, H. (1980) Screening of small molecular microbial products modulating immune responses and bestatin, *Recent Results Cancer Res. 75*, 115−125.
3. Taylor, A., Daims, M., Lee, J., and Surgenor, T. (1982) Identification and quantification of leucine aminopeptidase in aged normal and cataractous human lenses and ability of bovine lens LAP to cleave bovine crystallins, *Curr. Eye Res. 2*, 47−56.
4. Pulido-Cejudo, G., Conway, B., Proulx, P., Brown, R., and Izaguirre, C. A. (1997) Bestatin-mediated inhibition of leucine aminopeptidase may hinder HIV infection, *Antiviral Res. 36*, 167−177.
5. Carpenter, F. H., and Vahl, J. M. (1973) Leucine aminopeptidase (bovine lens). Mechanism of activation by Mg^{2+} and Mn^{2+} of the zinc metalloenzyme, amino acid composition, and sulfhydryl content, *J. Biol. Chem. 248*, 294−304.
6. Thompson, G. A., and Carpenter, F. H. (1976) Leucine aminopeptidase (bovine lens). The relative binding of cobalt and zinc to leucine aminopeptidase and the effect of cobalt substitution on specific activity, *J. Biol. Chem. 251*, 1618−1624.
7. Allen, M. P., Yamada, A. H., and Carpenter, F. H. (1983) Kinetic parameters of metal-substituted leucine aminopeptidase from bovine lens, *Biochemistry 22*, 3778−3783.
8. Sträter, N., and Lipscomb, W. N. (1995) Two-Metal Ion Mechanism of Bovine Lens Leucine Aminopeptidase: Active Site Solvent Structure and Binding Mode of L-Leucinal, a gem-Diolate Transition State Analog, by X-ray Crystallography, *Biochemistry 34*, 14792−14800.
9. Sträter, N., and Lipscomb, W. N. (1995) Transition State Analog L-Leucinephosphonic Acid Bound to Bovine Lens Leucine Aminopeptidase: X-ray Structure at 1.65 Å Resolution in a New Crystal Form, *Biochemistry 34*, 9200−9210.
10. Kim, H., and Lipscomb, W. N. (1993) X-ray crystallographic determination of the structure of bovine lens leucine aminopeptidase complexed with amastatin: Formulation of a catalytic mechanism featuring a gem-diolate transition state, *Biochemistry 32*, 8465−8478.
11. Burley, S. K., David, P. R., Sweet, R. M., Taylor, A., and Lipscomb, W. N. (1992) Structure determination and refinement of bovine lens leucine aminopeptidase and its complex with bestatin, *J. Mol. Biol. 224*, 113−140.
12. Ocain, T. D., and Rich, D. H. (1987) L-Lysinethiol: A subnanomolar inhibitor of aminopeptidase B, *Biochem. Biophys. Res. Commun. 145*, 1038−1042.
13. Chan, W. W.-C. (1983) L-Leucinthiol. A potent inhibitor of leucine aminopeptidase, *Biochem. Biophys. Res. Commun. 116*, 297−302.
14. Ocain, T. D., and Rich, D. H. (1988) Synthesis of sulfur-containing analogues of bestatin. Inhibition of aminopeptidases by α-thiol-bestatin analogues, *J. Med. Chem. 31*, 2193−2199.
15. Gordon, E. M., Godfrey, J. D., Delaney, N. G., Asaad, M. M., Von Langen, D., and Cushman, D. W. (1988) Design of novel inhibitors of aminopeptidases. Synthesis of peptide-derived diamino thiols and sulfur replacement analogs of bestatin, *J. Med. Chem. 31*, 2199−2211.
16. Beattie, R. E., Elmore, D. T., Williams, C. H., and Guthrie, D. J. (1987) The behavior of leucine aminopeptidase towards thionopeptides, *Biochem. J. 245*, 285−288.
17. Cappiello, M., Lazzaretti, A., Buono, F., Scaloni, A., D'Ambrosio, C., Amodeo, P., Mendez, B. L., Pelosi, P., Del Corso, A., and Mura, U. (2004) New role for leucyl aminopeptidase in glutathione turnover, *Biochem. J. 378*, 35−44.
18. Josch, C., Klotz, L. O., and Sies, H. (2003) Identification of cytosolic leucyl aminopeptidase (EC 3.4.11.1) as the major cysteinylglycine-hydrolyzing activity in rat liver, *Biol. Chem. 384*, 213−218.
19. Hanson, H., and Frohne, M. (1976) Crystalline leucine aminopeptidase from lens (α-aminoacyl-peptide hydrolase; EC 3.4.11.1), *Methods Enzymol. 45*, 504−520.
20. Bradford, M. M. (1976) A rapid and sensitive method for the quantitation of microgram quantities of protein utilizing the principle of protein-dye binding, *Anal. Biochem. 72*, 248−254.
21. Dixon, M. and Webb, E. C. (1979) Enzyme inhibition and activation, in *Enzymes*, 3rd ed., pp 332−467, Longman, London.
22. Otwinowski, Z., and Minor, W. (1997) Processing of X-ray diffraction data collected in oscillation mode, *Methods Enzymol. 276*, 307−326.
23. Brünger, A. T., Adams, P. D., Clore, G. M., De Lano, W. L., Gros, P., Grosse-Kunstleve, R. W., Jiang, J. S., Kuszewski, J., Nilges, M., Pannu, N. S., Read, R. J., Rice, L. M., Simonson, T., and Warren, G. L. (1998) Crystallography and NMR System: A new software suite for macromolecular structure determination, *Acta Crystallogr. D54*, 905−921.
24. Jones, T. A., Zou, J. Y., Cowan, S. W., and Kjeldgaard, M. (1991) Improved methods for building protein models in electron density maps and the location of errors in these models, *Acta Crystallogr. A47*, 110−119.
25. Engh, R. A., and Huber, R. (1991) Accurate bond and angle parameters for X-ray protein structure refinement, *Acta Crystallogr. A47*, 392−400.
26. Laskowski, R. A., MacArthur, M. W., Moss, D. S., and Thornton, J. M. (1993) PROCHECK: A program to check the stereochemical quality of protein structures, *J. Appl. Crystallogr. 26*, 283−291.
27. Case, D. A., Pearlman, D. A., Caldwell, J. W., Cheatham, T. E., III, Ross, W. S., Simmerling, C. L., Darden, T. A., Merz, K. M., Stanton, R. V., Cheng, A. L., Vincent, J. J., Crowley, M., Tsui, V., Radmer, R. J., Duan, Y., Pitera, J., Seibel, G. L., Singh, U. C., Weiner, P. K., and Kollman, P. A. (1999) *AMBER 6.0*, University of California, San Francisco.
28. Weiser, J., Shenkin, P. S., and Still, W. C. (1999) Approximate atomic surfaces from linear combinations of pairwise overlaps (LCPO), *J. Comput. Chem. 20*, 217−230.
29. Jorgensen, W. L., Chandrasekhar, J., Madura, J. D., Impey, R. W., and Klein, M. L. (1983) Comparison of simple potential functions for simulating liquid water, *J. Chem. Phys. 79*, 926−935.
30. Park, H., and Merz, K. M., Jr. (2005) Force Field Design and Molecular Dynamics Simulations of the Carbapenem- and Cephamycin-Resistant Dinuclear Zinc Metallo-β-lactamase from *Bacteroides fragilis* and Its Complex with a Biphenyl Tetrazole Inhibitor, *J. Med. Chem. 48*, 1630−1637.
31. Toba, S., Colombo, G., and Merz, K. M., Jr. (1999) Solvent Dynamics and Mechanism of Proton Transfer in Human Carbonic Anhydrase II, *J. Am. Chem. Soc. 121*, 2290−2302.
32. Stote, R. H., and Karplus, M. (1995) Zinc binding in proteins and solution: A simple but accurate nonbonded representation, *Proteins 23*, 12−31.
33. York, D. M., Darden, T. A., and Pedersen, L. G. (1993) The effect of long-range electrostatic interactions in simulations of macromolecular crystals: A comparison of the Ewald and truncated list methods, *J. Chem. Phys. 99*, 8345−8348.
34. Koradi, R., Billeter, M., and Wüthrich, K. (1996) MOLMOL: A program for display and analysis of macromolecular structures, *J. Mol. Graphics 14*, 51−55.
35. Borghi, C., Bacchelli, S., Degli Esposti, D., and Ambrosioni, E. A. (2004) A review of the angiotensin-converting enzyme inhibitor, zofenopril, in the treatment of cardiovascular diseases, *Expert Opin. Pharmacother. 5*, 1965−1977.
36. Lowther, W. T., and Matthews, B. W. (2002) Metalloaminopeptidases: Common functional themes in disparate structural surroundings, *Chem. Rev. 102*, 4581−4607.
37. Kim, H., and Lipscomb, W. N. (1993) Differentiation and identification of the two catalytic metal binding sites in bovine lens leucine aminopeptidase by X-ray crystallography, *Proc. Natl. Acad. Sci. U.S.A. 90*, 5006−5010.
38. Li, J.-Y., Chen, L.-L., Cui, Y.-M., Luo, Q.-l., Li, J., Nan, F.-J., and Ye, Q.-Z. (2003) Specificity for inhibitors of metal-substituted methionine aminopeptidase, *Biochem. Biophys. Res. Commun. 307*, 172−179.
39. Kishishita, S., Okajima, T., Kim, M., Yamaguchi, H., Hirota, S., Suzuki, S., Kuroda, S., Tanizawa, K., and Mure, M. (2003) Role of Copper Ion in Bacterial Copper Amine Oxidase: Spectroscopic and Crystallographic Studies of Metal-Substituted Enzymes, *J. Am. Chem. Soc. 125*, 1041−1055.
40. Holland, D. R., Hausrath, A. C., Juers, D., and Matthews, B. W. (1995) Structural analysis of zinc substitutions in the active site of thermolysin, *Protein Sci. 4*, 1955−1965.
41. Carpenter, F. H., and Vahl, J. M. (1973) Leucine aminopeptidase (Bovine lens). Mechanism of activation by Mg^{2+} and Mn^{2+} of

the zinc metalloenzyme, amino acid composition, and sulfhydryl content, *J. Biol. Chem. 248*, 294−304.
42. Aalbers, T. G., Houtman, J. P., and Makkink, B. (1987) Trace-element concentrations in human autopsy tissue, *Clin. Chem. 33*, 2057−2064.
43. Rasi, V., Costantini, S., Moramarco, A., Giordano, R., Giustolisi, R., and Gabrieli, C. B. (1992) Inorganic element concentrations in cataractous human lenses, *Ann. Ophthalmol. 24*, 459−464.
44. Stanojevic-Paovic, A., Hristic, V., Cuperlovic, M., Jovanovic, S., and Krsmanovic, J. (1987) Macro- and microelements in the cataractous eye lens, *Ophthalmic Res. 19*, 230−234.
45. Srivastava, V. K., Varshney, N., and Pandey, D. C. (1992) Role of trace elements in senile cataract, *Acta Ophthalmol. Scand. 70*, 839−841.
46. Çekiç, O., Bardak, Y., Totan, Y., Kavakli, S., Akyol, Ö., Özdemir, Ö., and Karel, F. (1999) Nickel, chromium, manganese, iron and aluminum levels in human cataractous and normal lenses, *Ophthalmic Res. 31*, 332−336.
47. Enoiu, M., Aberkane, H., Salazar, J. F., Leroy, P., Groffen, J., Siest, G., and Wellman, M. (2000) Evidence for the pro-oxidant effect of γ-glutamyltranspeptidase-related enzyme, *Free Radical Biol. Med. 29*, 825−833.
48. Dominici, S., Valentini, M., Mallearo, E., Del Bello, B., Paolicchi, A., Lorenzini, E., Tongiani, R., Comporti, M., and Pompella, A. (1999) Redox modulation of cell surface protein thiols in U937 lymphoma cells: The role of γ-glutamyl transpeptidase-dependent H_2O_2 production and S-thiolation, *Free Radical Biol. Med. 27*, 623−635.
49. Lou, M. F. (2003) Redox regulation in the lens, *Prog. Retinal Eye Res. 22*, 657−682.
50. Badiou, S., Bellet, H, Lehmann, S., Cristol, J.-P., and Jaber, S. (2005) Elevated plasma cysteinylglycine levels caused by cilastatin-associated antibiotic treatment, *Clin. Chem. Lab. Med. 43*, 332−334.

BI052069V